0022-3565/09/3311-77–86$20.00
THE JOURNAL OF PHARMACOLOGY AND EXPERIMENTAL THERAPEUTICS
JPET 331:77–86, 2009

Vol. 331, No. 1
155671/3517490
Printed in U.S.A.

Glyceraldehyde 3-Phosphate Dehydrogenase Depletion Induces Cell Cycle Arrest and Resistance to Antimetabolites in Human Carcinoma Cell Lines[S]

Manali S. Phadke, Natalia F. Krynetskaia, Anurag K. Mishra, and Evgeny Krynetskiy

School of Pharmacy (M.S.P., N.F.K., E.K.), and Jayne Haines Center for Pharmacogenomics and Drug Safety (N.F.K., A.K.M., E.K.), Temple University, Philadelphia, Pennsylvania

Received April 29, 2009; accepted July 21, 2009

ABSTRACT

Glyceraldehyde 3-phosphate dehydrogenase (GAPDH) is a multifunctional protein that acts at the intersection of energy metabolism and stress response in tumor cells. To elucidate the role of GAPDH in chemotherapy-induced stress, we analyzed its activity, protein level, intracellular distribution, and intranuclear mobility in human carcinoma cells A549 and UO31 after treatment with cytarabine, doxorubicin, and mercaptopurine. After treatment with cytosine arabinoside (araC), enzymatically inactive GAPDH accumulated in the nucleus. Experiments on fluorescence recovery after photobleaching with green fluorescent protein-GAPDH fusion protein in the live cells treated with araC demonstrated reduced mobility of green fluorescent protein-GAPDH inside the nucleus, indicative of interactions with nuclear macromolecular components after genotoxic stress. Depletion of GAPDH with RNA interference stopped cell proliferation, and induced cell cycle arrest in G_1 phase via p53 stabilization, and accumulation of p53-inducible CDK inhibitor p21. Neither p21 accumulation nor cell cycle arrest was detected in GAPDH-depleted p53-null NCI-H358 cells. GAPDH-depleted A549 cells were 50-fold more resistant to treatment with cytarabine (1.68 $\pm$ 0.182 μM versus 0.03 $\pm$ 0.015 μM in control). Depletion of GAPDH did not significantly alter cellular sensitivity to doxorubicin (0.05 $\pm$ 0.023 μM versus 0.035 $\pm$ 0.0154 μM in control). Induction of cell cycle arrest in p53-proficient carcinoma cells via GAPDH abrogation suggests that GAPDH-depleting agents may have a cytostatic effect in cancer cells. Our results define GAPDH as an important determinant of cellular sensitivity to antimetabolite chemotherapy because of its regulatory functions.

Glyceraldehyde 3-phosphate dehydrogenase (GAPDH) is recognized as an intriguing example of moonlighting proteins that perform multiple functions within seemingly unrelated pathways (Sirover, 2005). GAPDH was initially characterized as an enzyme involved in glucose metabolism converting glyceraldehyde 3-phosphate to 1, 3-diphosphoglycerate. Because cancer cells metabolize glucose mainly through the glycolytic pathway, and depend far less on oxidative phosphorylation (the Warburg effect), GAPDH is a central player in glycolysis-dependent energy supply, which places GAPDH at the core of cancer cell survival. Recent studies revealed the role of GAPDH as a signaling molecule that acts at the interface between stress factors and cellular apoptotic machinery (Colell et al., 2007; Nakajima et al., 2007; Sen et al., 2008). Because of these recently acknowledged facts, GAPDH is no longer a dull housekeeping protein; instead, it is engaged in multiple cytosolic and nuclear functions. Some of these functions could be cell-specific, because no moonlighting functions of GAPDH have been identified in lower eukaryotes (Gancedo and Flores, 2008).

This work was supported in part by the National Cancer Institute [Grant R01-CA104729]; by Jayne Haines Center for Pharmacogenomics and Drug Safety of Temple University School of Pharmacy; and by Temple University Summer Research Award (to E.K.).

The results of this study were presented in part at: Phadke M, Krynetskaia N, Krynetskiy E (2008) Glycolytic and nonglycolytic functions of GAPDH in cellular response to genotoxic drugs (Abstract), in *Proceedings of the 99th Annual Meeting of the American Association for Cancer Research*; 2008 April 12–16; San Diego, CA. Abstr 3341, American Association for Cancer Research, Philadelphia, PA. Phadke MS, Barrero C, Mishra A, Krynetskaia N, Merali S, Krynetskiy E (2009) Nuclear glyceraldehyde 3-phosphate dehydrogenase: a signaling molecule for cellular response to various anticancer drug therapies (Abstract), in *Proceedings of the 100th Annual Meeting of the American Association for Cancer Research*; 2009 April 18–22; Denver, CO. Abstr 3773, American Association for Cancer Research, Philadelphia, PA.

Article, publication date, and citation information can be found at http://jpet.aspetjournals.org.
doi:10.1124/jpet.109.155671.

[S] The online version of this article (available at http://jpet.aspetjournals.org) contains supplemental material.

ABBREVIATIONS: GAPDH, glyceraldehyde 3-phosphate dehydrogenase; FRAP, fluorescence recovery after photobleaching; NO, nitric oxide; araC, cytosine arabinoside, 4-amino-1-[(2*R*,3*S*,4*R*,5*R*)-3,4-dihydroxy-5- (hydroxymethyl)oxolan-2-yl] pyrimidin-2-one; MP, 6-mercaptopurine, 3,7-dihydropurine-6-thione; DOX, doxorubicin, (8*S*-*cis*)-10-[(3-amino-2,3,6-trideoxy-α-L-*lyxo*-hexopyranosyl)oxy]-7,8,9,10-tetrahydro-6,8,11-trihydroxy-8-(hydroxyacetyl)-1-methoxy-5, 12-naphthacenedione; MTT, 3-(4,5-dimethylthiazol-2-yl)-2,5-diphenyltetrazolium bromide; siRNA, short interfering RNA; siGAPDH, siRNAs targeted against GAPDH mRNA; CDK, cyclin-dependent kinase; DSB, double-strand break; GFP, green fluorescent protein; EGFP, enhanced green fluorescent protein; RNAi, RNA interference; Ab, antibody; PCA, personal cell analyzer.

The significance of GAPDH for chemotherapy remains obscure, although several lines of evidence suggest that GAPDH is involved in chemotherapy-induced DNA damage response. First, GAPDH catalyzes excision of uracil nucleobases from DNA, thus contributing to DNA repair activity (Meyer-Siegler et al., 1991). A recent study demonstrated the role of GAPDH in the repair of abasic sites in DNA (Azam et al., 2008). The intranuclear level of GAPDH correlates with the viability of human leukemia cells treated with MP; the higher level of intranuclear GAPDH significantly correlates with lower cell viability (Krynetski et al., 2001). Next, GAPDH was identified as a component of DNA-protein complexes formed on short DNA duplexes with inserted modified nucleosides araC, 5-fluorouracil, and MP (Krynetski et al., 2003). Finally, GAPDH forms complexes with DNA covalently linked to saframycin, a natural product with potent antiproliferative effect (Xing et al., 2004).

Genetic variations in the GAPDH gene family were associated with the late onset of Alzheimer's disease (Li et al., 2004). At least one genetic polymorphism, rs11549329, resulting in T99I mutation, is located in the vicinity of the NAD binding site, thus making it an intriguing target for pharmacogenetic studies.

In our study, we used human lung carcinoma A549 cells to explore the relationship between the level/activity of GAPDH and cellular response to genotoxic drugs. For the first time, our experiments demonstrated that the knockdown of GAPDH by RNA interference has a cytostatic effect in p53-proficient tumor cell, and that depletion of GAPDH dramatically increases the resistance of cells to the antimetabolite drug araC active in the S phase of the cell cycle. Our findings indicate that GAPDH is an important determinant of cancer cell proliferation, and a modulator of cellular response to chemotherapeutic agents.

Materials and Methods

Cell Cultures, Drug Treatment, and Plasmids. Lung carcinoma cells A549 and NCI-H358 were obtained from the American Type Culture Collection (Manassas, VA), and renal carcinoma UO31 cells were obtained from the Tumor Cell Line Repository, National Cancer Institute (Frederick, MD). A549 cells were maintained in Ham's F-12K medium, and NCI-H358 and UO31 cells were maintained in RPMI 1640 medium (American Type Culture Collection) at 40 to 80% confluence. Cells were treated with drugs dissolved in 0.1 N NaOH (mercaptopurine, MP), or water (cytarabine, araC) as 500 to 1000× stock solutions; drug concentrations were determined spectrophotometrically (MP, ε_{320} = 19,600; araC, ε_{272} = 9259) (O'Neil et al., 2001). [5-^{3}H]Cytosine-β-D-arabinofuranoside (14.9 Ci/mmol) (Moravek Biochemicals, Brea, CA) was used in DNA incorporation experiments (Krynetskaia et al., 2009). Human GAPDH cDNA was inserted in frame with EGFP into pcDNA3.1 as described previously (Brown et al., 2004) and verified by sequencing.

Cell Growth and Viability. Cell viability and cell count were determined by flow cytometry by use of ViaCount reagent with Guava Personal Cell Analyzer (Guava Technologies, Hayward, CA). For the 3-(4,5-dimethylthiazol-2-yl)-2,5-diphenyltetrazolium (MTT) assay (CellTiter 96 cell proliferation kit; Promega, Madison, WI), A549 cells (250 cells per well) were plated into 96-well plates and cultured for 3 to 5 days in varying concentrations of the following drugs: 0 to 100 μM araC or MP. After incubation, MTT reagent was added to each well, and endpoint data were collected by an M2 microplate spectrophotometer (Molecular Devices, Sunnyvale, CA) according to the manufacturer's instructions. The IC_{50} values were calculated by use of GraphPad Prism (GraphPad Software Inc., San Diego, CA) by fitting a sigmoid E_{max} model to the cell viability versus drug concentration data, as determined in duplicate from three independent experiments.

Cell cycle analysis was performed by use of the cell cycle kit according to manufacturer's protocol (Guava Technologies). In brief, 5×10^5 to 1×10^6/ml cells were trypsinized, centrifuged, and resuspended in 30 ml of ice-cold 70% ethanol. After incubation for 12 h at 4°C, 1×10^5 to 2×10^5 ethanol-fixed cells were centrifuged at 450*g* for 5 min, washed with phosphate-buffered saline, and resuspended in 200 μl of Guava Cell Cycle Reagent, and incubated for 30 min at room temperature. The data were collected and analyzed by a Guava personal cell analysis (PCA) flow cytometer with use of CytoSoft software (Guava Technologies). Approximately 10,000 cells were analyzed in each experiment.

Transfection with GFP-GAPDH and Fluorescence Recovery after Photobleaching Experiments. Approximately 25,000 cells per dish were seeded in 35-mm glass-bottom Petri dishes (MatTek, Ashland, MA) and transfected with pEGFP (Clontech, Mountain View, CA) or pEGFP-GAPDH plasmid by use of FuGene6 transfection reagent (Roche Molecular Systems Inc., Branchburg, NJ). The next day, cells were treated with 10 μM araC and incubated for 24 h. After incubation, fluorescence recovery after photobleaching (FRAP) experiments were performed on a Leica TCS SP2 AOBS confocal microscope equipped with a 63×/1.4 N.A. oil immersion objective at 37°C. Prebleaching plateau was defined by acquiring 20 single-section images with 6× zoom on an area 7 × 7 μm, with acquisition speed 287 ms/frame. Bleaching was performed with three pulses using the 458, 476, and 488 nm lines of the Ar laser. Fluorescence recovery was monitored collecting 40 single-section images at 287-ms intervals with low laser intensity (5% of the bleach intensity with the single 488-nm laser line; detection, 495–600 nm). Quantitative analysis was performed after background subtraction, correction for laser fluctuations, and acquisition photobleaching, and normalization as described by Rabut and Ellenberg (2005). Five to ten cells were analyzed on each dish; all experiments were repeated four to five times. Diffusion coefficient D value was calculated according to Axelrod et al. (1976) by use of the equation $D = 0.88 \cdot w^2/(4t_{½})$, where w is a radius of bleached area, with the assumptions that the bleached area is a disc and that diffusion occurs only laterally. The immobile fraction was calculated as a ratio of the final to the initial fluorescence intensity after correction for loss of signal due to photobleaching (Rabut and Ellenberg, 2005).

Isolation of Subcellular Fractions. Separation of cytosolic and nuclear fractions was performed with NE-PER Nuclear and Cytoplasmic Extraction kit (Thermo Fisher Scientific, Rockford, IL), per manufacturer's instructions. In brief, A549 cells (1 to 2×10^6 cells) were trypsinized, and 100 μl of cytoplasmic extraction reagent I supplemented with protease inhibitor (Sigma-Aldrich, St. Louis, MO) was added to the cell pellet, vortexed, and incubated on the ice for 10 min. Next, 5.5 μl of cold cytoplasmic extraction reagent II was added to the tube, incubated on the ice for 1 min, and centrifuged at 4°C at 16,000*g* for 5 min. The supernatant (cytoplasmic fraction) was immediately transferred into a prechilled tube. The pellet of nuclei was resuspended in a cold mixture of 50 μl of nuclear extraction reagent supplemented with 1 μl of protease inhibitor, and vortexed every 10 min for 40 min. The tube was centrifuged at 4°C at 16,000*g* for 10 min, and the supernatant (nuclear extract) was transferred to a prechilled tube. The extracts were snap-frozen on dry ice and stored at −80°C.

RNA Interference with Short Duplex RNA. RNAi experiments were performed by use of the predesigned Stealth RNA (GAPDH Validated Stealth RNAi DuoPak duplexes 1 and 2, and CDKN1A Validated Stealth RNAi DuoPak duplexes 1 and 2) (Invitrogen, Carlsbad, CA). Transient transfection was performed in T25 flasks plated at a density of 1.4×10^4 cells/cm^2 with use of Lipofectamine 2000 transfection reagent, according to the manufacturer's instructions. Transfection was repeated the next day. After 48-h incubation, cells were trypsinized and

seeded in T75 flasks for drug treatment. The final concentration of siGAPDH was 20 to 145 nM; the concentration of siCDKN1A was 10 nM. Scrambled Negative Stealth RNAi control (Invitrogen) was used as negative control in all siRNA experiments.

Analysis of mRNA Expression by Real-Time Polymerase Chain Reaction. Total cellular RNA was extracted with TriReagent (Invitrogen) from A549 and UO31 cells (approximately 5×10^6 cells per experiment, three replicates). Approximately 500 ng of total RNA was reverse transcribed by use of the TaqMan Reverse Transcription kit (Applied Biosystems, Foster City, CA) according to the manufacturer's instructions. The level of mRNA was evaluated with use of the relative quantification protocol with human β-actin as a normalization standard on an ABI 7300 real time polymerase chain reaction instrument (Applied Biosystems) according to manufacturer's instructions. Data were collected from three independent experiments for each sample.

Western blot analysis was performed as described earlier (Krynetskaia et al., 2009). In brief, 1 to 2×10^6 control and treated cells were trypsinized, counted with ViaCount reagent by use of Guava PCA flow cytometer (Guava Technologies); cells were collected by centrifugation at 500*g* for 5 min at 4°C. Total cellular extract was prepared by lysis in radioimmunoprecipitation assay buffer with protease and phosphatase inhibitors (Santa Cruz Biotechnology, Santa Cruz, CA). The protein concentration was determined in cellular extracts by use of PlusOne2D Quant kit (GE Healthcare, Little Chalfont, Buckinghamshire, UK). Electrophoretic separation was performed by use of 16% polyacrylamide gels for analysis of γH2AX; 12% polyacrylamide gels for analysis of p53, phosphorylated p53, GAPDH, and β-actin (PAGEGel, San Diego, CA). Forty micrograms of total protein was loaded per lane, and transferred to a nitrocellulose membrane (PAGEGel) in a Mini Trans-Blot electrotransfer cell (Bio-Rad Laboratories, Hercules, CA). Membranes were developed with rabbit polyclonal anti-GAPDH Ab at 1:10,000 dilution (Santa Cruz, Santa Cruz, CA); rabbit anti-Ser15-phosphorylated p53 Ab at 1:1000 dilution and rabbit anti-γH2AX (H2AX phosphorylated at Ser139) polyclonal Ab at 1:500 dilution (Calbiochem, La Jolla, CA), mouse anti-p53 monoclonal Ab at 1:500 dilution (Santa Cruz Biotechnology), mouse anti-p21 monoclonal Ab at 1:50 dilution (Santa Cruz Biotechnology), and mouse anti-β-Actin monoclonal Ab at dilution 1:10,000 (Sigma-Aldrich). Bands were visualized by treatment with secondary antibody: IRDye680 donkey anti-mouse antibody and IRDye680 goat anti-rabbit antibody, or IRDye 800CW donkey anti-rabbit antibody (LI-COR Biosciences, Lincoln, NE) and IRDye 800CW goat anti-rat antibody (Rockland Immunochemicals, Gilbertsville, PA) at 1:10,000 dilution. Anti-β-actin antibody was used for evaluating loading controls. Bands were visualized and quantified by Odyssey Infrared Imaging system (LI-COR Biosciences) with use of two-color fluorescence detection at 700 and 800 nm.

Neutral Comet Assay. DSBs were detected by Neutral Comet assay with the CometAssay kit (Trevigen, Gaithersburg, MD), according to the manufacturer's instructions. In brief, approximately 350,000 cells were exposed to one of the following agents: 200 μM H_2O_2 for 20 min, 1 μM DOX for 18 h, 1 μM araC for 24 h. Cells were collected by trypsinization, mixed with low-melting-point agarose (1:10 v/v), and applied on the Fragment Length Analysis using Repair Enzymes (FLARE) slides (Trevigen). After cell lysis in a neutral lysis buffer at 4°C overnight, slides were rinsed with 1× 89 mM Tris borate/2 mM EDTA buffer and subjected to electrophoresis at 1 V/cm for 20 min. Slides were rinsed with distilled water, fixed with 70% ethanol for 5 min, and air-dried. After staining with SYBR Green, images were recorded by use of a Nikon Eclipse 50 fluorescent microscope equipped with a CCD camera, and analyzed with CometScore freeware (TriTek, Sumerduck, VA). The Olive Tail Moment was determined for 50 cell images in each sample (Olive et al., 1991).

GAPDH Activity. GAPDH enzymatic activity was estimated with KDalert GAPDH Assay (Ambion, Austin, TX). Increase in fluorescence was measured by use of SpectraMax M2 spectrofluorometer (Molecular Devices) with excitation at 560 nm and emission at 590 nm, and quantified against the calibration curve.

Caspase Activity. Caspase activity was assessed by use of fluorogenic substrates for caspase 3 and caspase 7 with Apo-ONE Homogenous Caspase 3/7 Assay as described by Krynetskaia et al. (2009).

Statistical Analysis. The statistical analyses were performed by use of Student's *t* test with Statistica software program (StatSoft, Tulsa, OK), and nonlinear regression analysis with GraphPad Prizm 4.0 software (GraphPad Software). A p value of <0.05 was considered statistically significant. Data are presented as the mean ± S.E.

Results

AraC Treatment of A549 Cells Causes Cytotoxicity, Accumulation of DSBs in DNA, and Phosphorylation of p53 and H2AX. In our experiments, human carcinoma cell line A549 expressing functional p53 was found to be sensitive to araC (0–50 μM, IC_{50} 0.03 ± 0.015 μM) and resistant to MP treatment (0–100 μM, $IC_{50} > 100$ μM), as revealed by MTT assay (Fig. 1A). Evaluation of DNA integrity by use of the Comet assay demonstrated accumulation of DSBs in DNA of araC-treated cells, whereas a significantly lower level of DSBs was detected in control or MP-treated cells (Fig. 1B). Western blot analysis showed accumulation of p53-Ser15 (p53 phosphorylated at Ser 15) and γH2AX (H2AX phosphorylated at Ser 139), two well-characterized markers of DNA damage, after treatment with araC, but not after treatment with MP (Fig. 1, C and D).

Intranuclear Accumulation of GAPDH in Response to Genotoxic Stress Is Accompanied by Reduction of Nuclear GAPDH Activity. In unstressed cells GAPDH was localized in the cytosol and excluded from the nucleus, as evidenced by Western blot analysis (Fig. 2A). After 24 h of treatment with chemotherapeutic agents, araC or MP, GAPDH protein accumulated in the nuclear compartment. In contrast to araC treatment, MP caused reversible intranuclear accumulation of GAPDH (Fig. 2A). No change in the level of cytosolic GAPDH protein was detected by Western blot analysis (not shown).

By use of confocal microscopy, we monitored the distribution of EGFP-GAPDH fluorescent protein between cellular compartments in the live cells, before and after araC treatment. Two fluorescent proteins, EGFP and EGFP-GAPDH, were distributed differently inside the live cells. In untreated cells, EGFP evenly filled both cytosolic and nuclear compartments of A549 cells (Supplemental Fig. S1A). In contrast, EGFP-GAPDH had primarily cytosolic localization and was excluded from nuclei (Fig. 3C). Genotoxic stress caused by araC treatment did not alter the distribution of EGFP between nuclear and cytosolic fractions (Supplemental Fig. S1C), whereas GFP-GAPDH was accumulated in the nuclei after exposure to 10 μM araC for 24 h (Fig. 3D). Consistent with the results of Western blot analysis, MP treatment (which was not cytotoxic for A549) resulted in intranuclear accumulation of EGFP-GAPDH (Fig. 2, A and E).

To characterize catalytic properties of intranuclear GAPDH, we evaluated the protein level and glycolytic activity of GAPDH in nuclei and cytosol of the cells after antimetabolite treatment. Specific activity of nuclear GAPDH in A549 cells normalized per intranuclear GAPDH protein level was decreased after araC treatment; in contrast, noncytotoxic MP treatment caused intranuclear accumulation of GAPDH, but did not reduce enzymatic activity (Fig. 2B).

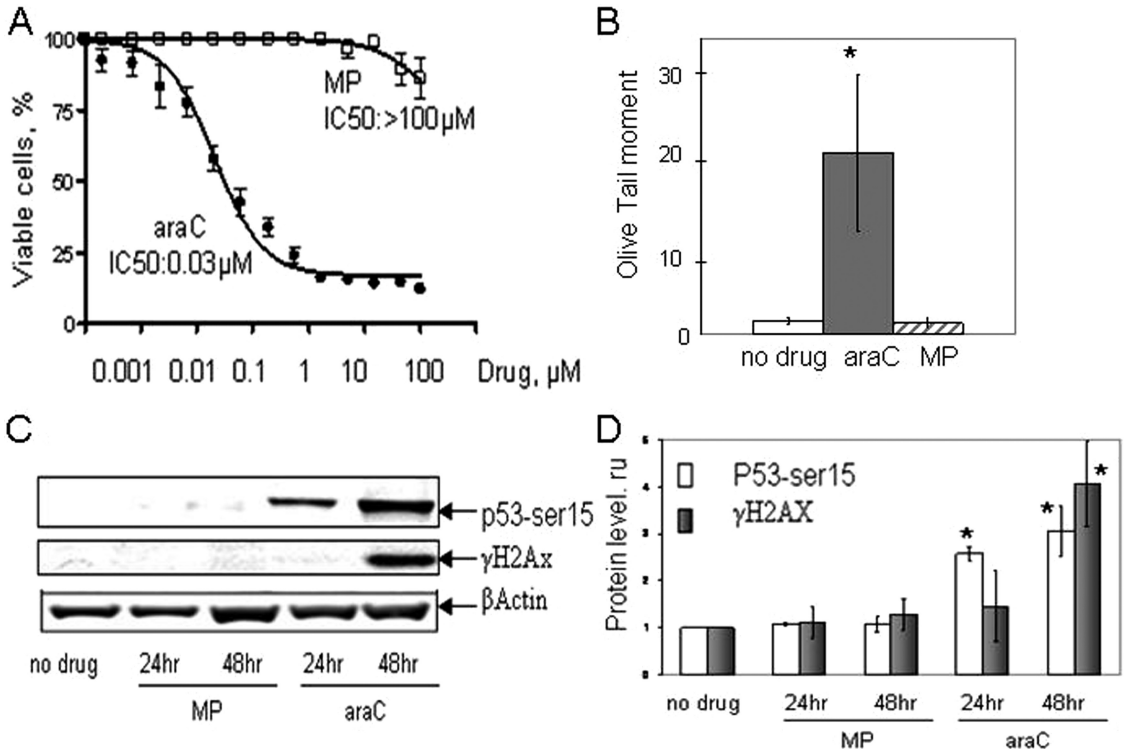

Fig. 1. Chemosensitivity of human carcinoma A549 cells to antimetabolite drugs araC and MP correlates with DNA damage, and phosphorylation of p53 and H2AX. A, cytotoxic/cytostatic effect of antimetabolites (●, araC; □, MP) evaluated by MTT assay. A549 cells were plated into 96-well plates (250 cells per well), and cultured for 5 days in varying concentrations (0–100 μM) of araC or MP. Curves represent the results of three independent experiments, with two duplicates in each experiment. B, Comet assay analysis of DSBs in DNA of A549 cells after antimetabolite treatment. After electrophoresis, cells were stained with SYBR Green, and the Olive Tail Moment was determined for 50 cells as described under *Materials and Methods*. C, treatment of A549 cells with araC, but not MP, induced accumulation of stress markers S15-phosphorylated p53 (p53-Ser15) and S139-phosphorylated H2AX (γH2AX). β-Actin was used as a normalization standard. D, Western blot membrane shown in C was quantified by use of the Odyssey LI-COR Imaging system, as described under *Materials and Methods*. p53-Ser15 (□); γH2AX (■). *, $p < 0.05$ in comparison with no drug control.

FRAP Experiments Revealed Reduced Mobility of GAPDH in the Nucleus. We evaluated dynamic properties of fluorescent proteins in the cytosolic and nuclear compartments of the live cells by use of the FRAP technique (Phair and Misteli, 2000). The recovery of fluorescence intensity in the cytosolic and nuclear compartments was measured after short-term photobleaching of the preselected spots inside the cytosolic or nuclear areas of the cell, before and after drug treatment (Fig. 2 and Supplemental Fig. S1). Recovery of the fluorescent signal for EGFP protein was fast and reached a plateau after approximately 20 s. The diffusion coefficient D values for the cytosolic and nuclear EGFP were similar (Table 1). The high percentage of recovery of fluorescence in the cells expressing EGFP indicated the low level of the immobile fraction ($1 - M_f$) (Supplemental Fig. S1B). After treatment with MP (which was not cytotoxic for A549 cells), the D value of the nuclear EGFP-GAPDH was similar to that of cytosolic form of EGFP-GAPDH (Fig. 2E; Table 1). In contrast, recovery of fluorescence in the nuclear and cytosolic fractions of EGFP-GAPDH after araC treatment occurred differently. Nuclear EGFP-GAPDH had an approximately 4 times lower D value compared with cytosolic EGFP-GAPDH, and the immobile fraction ($1 - M_f$) of nuclear EGFP-GAPDH molecules was higher (Fig. 2D; Table 1).

Knockdown of GAPDH Results in Reduced Cell Proliferation and Cell Cycle Arrest in p53-Proficient Cells. Human carcinoma cell lines A549 and UO31 expressing functional p53 were transiently transfected with two different siRNAs targeted against GAPDH mRNA (siGAPDH) as described under *Materials and Methods*. The level of GAPDH mRNA in both siGAPDH-treated cell lines was reduced to 5 to 10% of control, and the content of GAPDH protein was reduced to 10 to 30% of the basal level (Supplemental Fig. S2, A, B, and D). Consistent with this decrease in protein level, GAPDH activity dropped to 20 to 40% of control in A549 and UO31 cells (Supplemental Fig. S2C). The reduced level of GAPDH protein was not restored until 6 days after transfection (Supplemental Fig. S3).

Depletion of GAPDH after transient transfection with siGAPDH arrested cell proliferation, as shown on Fig. 3A; a similar result achieved in the UO31 cell line (data not shown). There was no cell growth arrest in control cells transfected with scrambled siRNA (Fig. 3). Cell cycle analysis of A549 revealed that the GAPDH-depleted cells accumulated in the G_0/G_1 phase, with corresponding decrease of cells in S and G_2/M phase (Fig. 4): percentage of A549 cells in the G_0/G_1 phase increased from 57 to 77%; in the S phase, the percentage dropped from 12 to 6%; in the G_2/M phase, it dropped from 22 to 11% ($p < 0.002$). Upon incubation of GAPDH-depleted cells with [^{3}H]araC, we detected incorporation of radioactivity into DNA. The level of radioactivity in DNA further increased after 48 h of incubation in both control and GAPDH-depleted cells, indicating DNA polymerase activity in the cells (Fig. 4B).

To compensate for the requirements for glycolytic functions of GAPDH, the cells were routinely maintained in pyruvate-containing medium (Zheng et al., 2003). We did not find differences

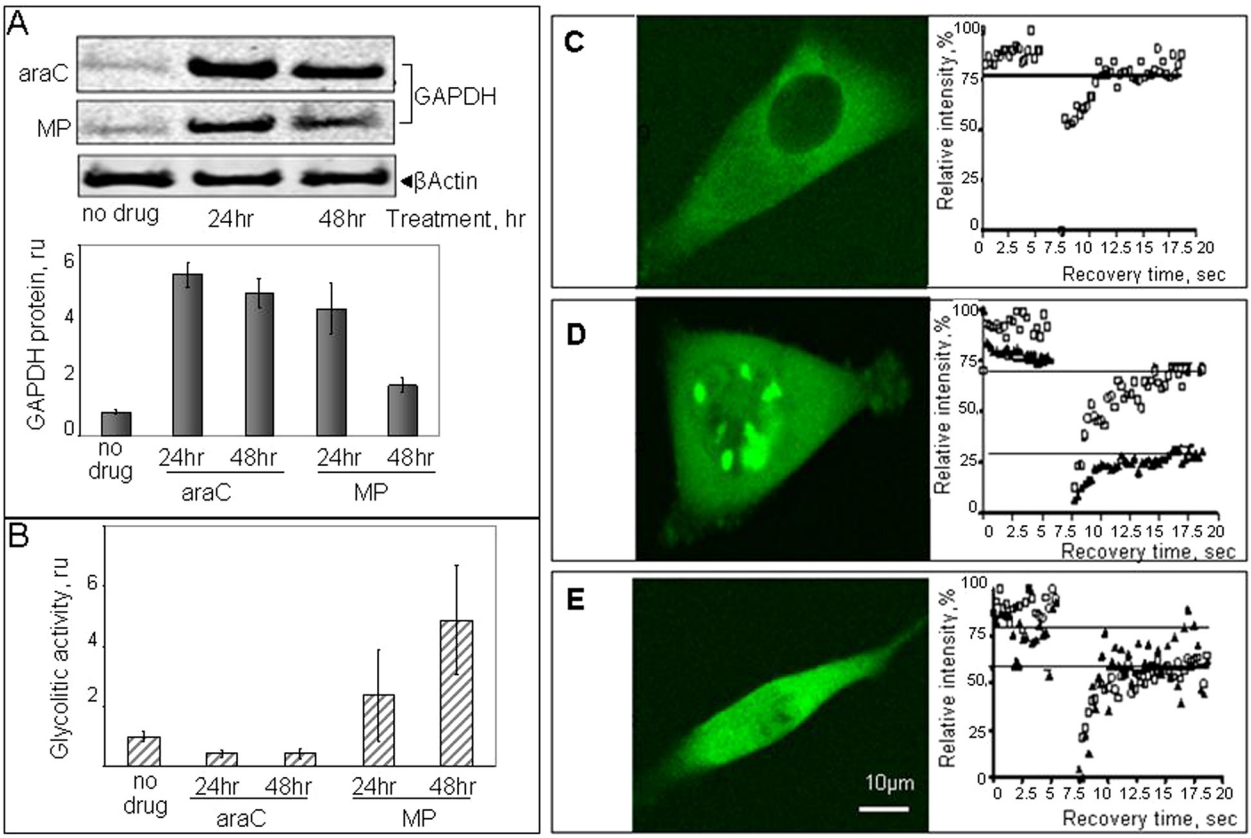

Fig. 2. AraC-induced genotoxic stress changes the level, glycolytic activity, and mobility of GAPDH protein in the nuclear compartment. A, intranuclear accumulation of GAPDH after incubation with antimetabolite drugs was demonstrated by Western blot analysis of nuclear extracts from A549 cells treated with 1 μM araC (top blot), or 10 μM MP (middle blot) for 24 to 48 h. Relative level of nuclear GAPDH protein was estimated by image analysis of membranes after staining with infrared dye-labeled antibodies. β-Actin was used as normalization standard. B, nuclear GAPDH activity after cell incubation with antimetabolite drugs was estimated by fluorescent assay, as described under *Materials and Methods*. Results of the assay were quantified against a standard enzyme preparation provided in the kit. C to E, molecular dynamics of fluorescent protein EGFP-GAPDH in subcellular compartments of A549 cells. A549 cells were transiently transfected with EGFP-GAPDH-encoding plasmid and treated with araC or MP. Confocal imaging and evaluation of recovery after photobleaching of EGFP-GAPDH fusion protein were performed in transfected cells before treatment (C), after treatment with 10 μM araC for 24 h (D), and after treatment with 50 μM MP for 24 h (E). □, cytosolic EGFP-GAPDH; ▲, nuclear EGFP-GAPDH. The diffusion coefficients *D* calculated from FRAP experiments, as described under *Materials and Methods*, are shown in Table 1.

in cell proliferation between GAPDH-depleted cells grown in the regular medium and the medium supplemented with 1 mM sodium pyruvate ($p > 0.5$) (Supplemental Fig. S4A).

Depletion of GAPDH Induces Cell Cycle Arrest via Activation of p53 and Accumulation of CDK Inhibitor p21. The cell cycle arrest in GAPDH-depleted cells was accompanied by accumulation of p53 and CDK inhibitor p21, as revealed by Western blot analysis (Fig. 3B, Supplemental Fig. S4B). We used p53-null human carcinoma cells NCI-H358 to test the hypothesis that the cell proliferation arrest after GAPDH knockdown occurs via p53-dependent activation of p21. NCI-H358 cells do not express p53 under normal conditions or after GAPDH knockdown (Fig. 3B). Knockdown of GAPDH in NCI-H358 cells did not induce p21, in contrast to p53-proficient A549 cells (Fig. 3B). NCI-H358 cells with depleted GAPDH continued proliferation but at lower rate compared with control cells (Fig. 3A). In A549 cells simultaneously treated with siGAPDH and sip21, the accumulation of p21 was significantly lower compared with cells treated with siGAPDH alone; these cells continued proliferation at a reduced rate (Fig. 3D).

Carcinoma Cells with Low GAPDH Level Manifest Increased Chemoresistance to araC Treatment. The cytotoxic/cytostatic effects of araC and DOX in control cells and cells with knocked-down GAPDH were evaluated with the MTT assay. A549 cells with a reduced level of GAPDH were approximately 50 times less sensitive to araC treatment compared with cells transfected with scrambled siRNA (Fig. 5A). In contrast, cytotoxicity of DOX (a cytotoxic agent with a different mechanism of action) in GAPDH-depleted A549 cells was similar to that in control cells (Fig. 5B). Both araC and DOX caused formation of DSBs in DNA of the treated cells, as shown on Fig. 4C. Accumulation of DSBs in DNA of GAPDH-depleted cells after araC treatment was significantly lower compared with control cells transfected with scrambled siRNA, as estimated by the neutral Comet assay; there was no difference after DOX treatment (Fig. 4C). Caspase 3/7 activation and H2AX phosphorylation after araC were also significantly lower in GAPDH-depleted cells, whereas the effects of DOX treatment in GAPDH-proficient and -deficient cells did not differ significantly (Fig. 5, C and D).

Discussion

In this study, we focused on the role of GAPDH in cellular response to genotoxic stress inflicted by anticancer drugs: pyrimidine nucleoside antimetabolite araC and Topo II inhibitor DOX. Both drugs have been used in anticancer che-

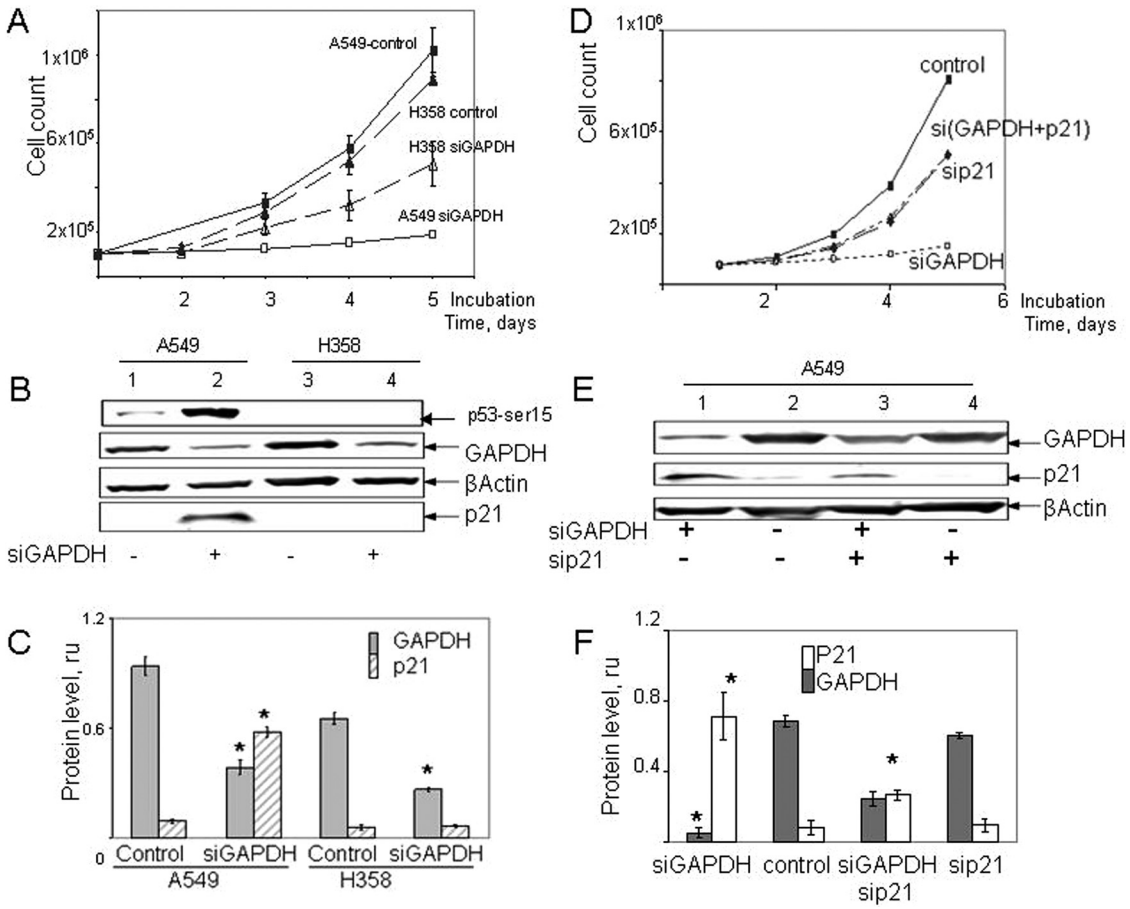

Fig. 3. Knockdown of GAPDH induces cell growth arrest via phosphorylation of p53, and induction of CDK inhibitor p21 in cells proficient in p53 and p21 proteins. A, GAPDH depletion induces cell growth arrest in A549 cells but not in NCI-H358 cells. After transfection with siGAPDH, cells were incubated for 48 h, seeded in 12-well plates at a density of 12,500 cells/cm^2, collected every 24 h by trypsinization, and counted by use of Guava PCA flow cytometer as described under *Materials and Methods*. Scrambled siRNA was used as a control in all experiments. B, GAPDH knockdown with siGAPDH resulted in p53 phosphorylation at Ser15, and accumulation of CDK inhibitor p21 in A549, but not in NCI-H358 cells. β-Actin, loading control. C, Western blot membrane shown in B was quantified by use of Odyssey LI-COR Imaging system, as described under *Materials and Methods*. ▨, GAPDH protein level; ▨, p21 protein level. ∗, $p < 0.05$ in comparison with no drug control. D, knockdown of p21 in GAPDH-depleted A549 cells abrogated cell proliferation arrest. After transfection with siRNA (■, control; ♦, sip21; □, siGAPDH; +, cotransfection with siGAPDH and sip21), A549 cells were incubated for 48 h, seeded in 12-well plates at a density of 12,500 cells/cm^2, collected every 24 h by trypsinization, and counted by use of Guava PCA flow cytometer as described under *Materials and Methods*. E, knockdown of p21 in GAPDH-depleted cells in the experiment shown in D was demonstrated by Western blot analysis. Antibodies to GAPDH and p21 were used for detection and quantification of residual protein. β-Actin, loading control. Scrambled siRNA was used as negative control. F, Western blot membrane shown in F was quantified by use of Odyssey LI-COR Imaging system, as described under *Materials and Methods*. □, p21 protein level; ▨, GAPDH protein level. ∗, $p < 0.05$ in comparison with control (lane 2).

TABLE 1

Molecular dynamics parameters of EGFP and EGFP-GAPDH fusion protein estimated by FRAP analysis of transiently transfected A549 cells

The value of the diffusion coefficient D was calculated under the assumption that the bleached area is a disc and that diffusion occurs only laterally (Axelrod, et al., 1976).

Protein	Cellular Compartment	Drug Treatment	Immobile Fraction, $(1 - M_f)$	t[1/2]	D
				s	$\mu m^2/s$
EGFP	Cytosol	No drug	0.19	0.67	4.0
EGFP	Nuclei	No drug	0.23	0.65	4.2
EGFP	Cytosol	araC	0.19	0.45	6.0
EGFP	Nuclei	araC	0.34	0.68	4.0
EGFP-GAPDH	Cytosol	No drug	0.24	0.67	4.0
EGFP-GAPDH	Cytosol	araC	0.25	0.80	3.4
EGFP-GAPDH	Nuclei	araC	0.75	2.64	1.0
EGFP-GAPDH	Cytosol	MP	0.26	0.60	4.5
EGFP-GAPDH	Nuclei	MP	0.34	0.70	3.9

motherapy for several decades, although the details of their cytotoxic effects remain to be elucidated. A general mechanism of cytotoxicity of araC is incorporation of nucleoside analogs into DNA catalyzed by DNA polymerase; DOX directly introduces DSBs by inhibiting topoisomerase II reaction. It is noteworthy that araC causes cell cycle arrest in the S phase and cell death via a p53-dependent intrinsic apoptotic pathway accompanied by induction of caspase 3 which is pathognomonic for classical apoptosis (Sampath et al., 2003). The results of our present experiments showing that, in A549

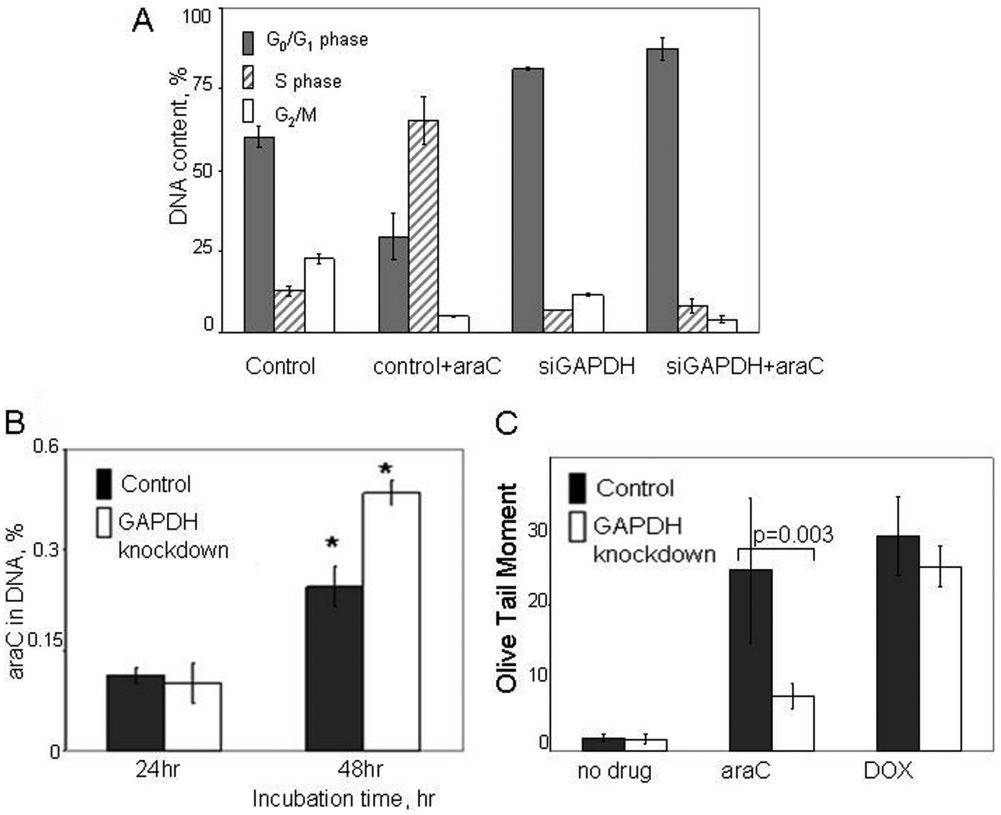

Fig. 4. AraC treatment has differential effects in GAPDH-proficient and -deficient cells. A, after araC treatment, GAPDH-proficient, but not GAPDH-depleted A549 cells accumulate in the S phase. After araC treatment, actively dividing control cells underwent cell cycle arrest in the S phase, whereas GAPDH-depleted cells did not manifest a change in cell cycle distribution. Cell cycle analysis was performed with the Guava Cell Cycle reagent kit. Cells were incubated 48 h after transfection, replated, and treated with 1 μM araC for 24 h. The number of cells in each phase was estimated by use of CytoSoft software. In each experiment, 10,000 cells were collected for cell cycle analysis. B, GAPDH depletion does not inhibit DNA polymerase activity and incorporation of araC in DNA. A549 cells transiently transfected with scrambled siRNA (control, ■) or siGAPDH (GAPDH knockdown, □) were incubated for 48 h, and treated with [^{3}H]araC for 24 to 48 h at a final concentration of 1 μM as described earlier (Krynetskaia et al., 2009). DNA was extracted from the cells by use of DNAamp DNA Minikit (QIAGEN, Valencia, CA) and quantified by UV spectroscopy, and ^{3}H incorporation into DNA was determined by liquid scintillation counting. C, GAPDH depletion reduces the level of DNA damage in A549 cells induced by araC but not DOX treatment. Accumulation of DSBs in DNA of control (■) and GAPDH-depleted cells (□) was estimated by use of neutral Comet assay analysis. After electrophoresis, cells were stained with SYBR Green, and the Olive Tail Moment was determined for 50 cells in each sample as described under *Materials and Methods*.

cells, araC acts thorough p53-apoptotic pathway accompanied by p53 phosphorylation, increase of γH2AX level, and caspase activation are in line with these findings (Krynetskaia et al., 2009). Caspase 3 activation is not required for necrosis, and occurs very late or not at all in autophagy; it might therefore differentiate between these modes of cell death (Braess et al., 2004; Levine and Yuan, 2005).

An intriguing feature of GAPDH is its intranuclear accumulation in response to nongenotoxic and genotoxic stimuli. Supplemental Table S1 summarizes the stress factors promoting intranuclear GAPDH accumulation. Earlier we demonstrated the CRM1-dependent mechanism of intranuclear GAPDH accumulation based on the interaction between CRM1 and the nuclear export signal of GAPDH. GAPDH variants with mutated nuclear export signal showed intranuclear localization in the absence of stress stimuli (Brown et al., 2004). An alternative NO-dependent mechanism of GAPDH intranuclear localization was suggested by Sawa and coworkers (2008) who demonstrated *S*-nitrosylation at the active-site Cys residue in GAPDH; *S*-nitrosylated GAPDH binds Siah1 ligase and relocates into the nucleus (Hara et al., 2005). This mechanism implies that intranuclear translocation induced by *S*-nitrosylation results in accumulation of enzymatically inactive GAPDH in the nucleus (Molina y Vedia et al., 1992). Consistent with this mechanism, we observed accumulation of inactive GAPDH in the nuclei of araC-treated A549 cells (Fig. 2, A and B). We were surprised to find that treatment of A549 cells with MP, which is not cytotoxic for this cell line, resulted in intranuclear accumulation of enzymatically active GAPDH (Fig. 2, A and B). MP was not cytotoxic for A549 up to 100 μM; no accumulation of DSBs in DNA, or stress markers p53-Ser 15 and γH2AX, were detected after MP treatment (Fig. 1, B–D). Therefore, intranuclear accumulation of GAPDH may occur without genotoxic stress, via NO-independent mechanism without affecting GAPDH catalytic activity. Although the residual level of GAPDH after transient transfection with siGAPDH was between 10 and 30%, we did not observe intranuclear accumulation of GAPDH in GAPDH-depleted cells after araC treatment (data not shown).

To assess GAPDH functions in cellular response to antimetabolites, we monitored its intranuclear mobility inside the live cells after drug treatment, and evaluated its role in drug response by use of human carcinoma cells A549 where GAPDH was depleted by transient transfection with siRNA. Because GAPDH was excluded from the nuclei of unstressed cells (Fig. 2C), we compared the mobility of EGFP-GAPDH in

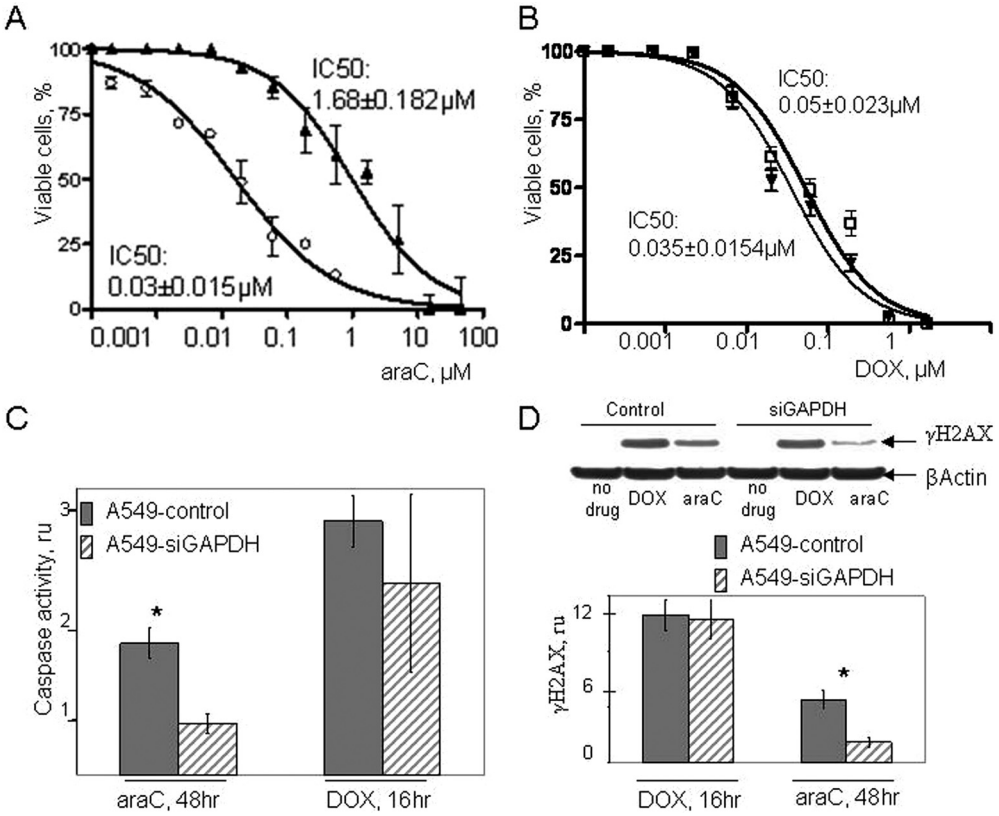

Fig. 5. GAPDH-depleted A549 cells revealed increased resistance to the antimetabolite drug araC but not DOX. A and B, comparison of cytotoxic/cytostatic effects of araC and DOX in GAPDH-proficient versus GAPDH-deficient A549 cells. After transfection with siRNA (○, □, scrambled siRNA; ▲, ▼, siGAPDH), A549 cells were plated into 96-well plates (250 cells per well), cultured for 3 days in 0 to 100 μM araC (A) or 0 to 2 μM DOX (B), and their chemosensitivity was evaluated by MTT assay. Curves represent the results of three independent experiments, with two duplicates in each experiment. Where not seen, the error bars are smaller than the data point symbols. C, caspase activation after araC treatment is inhibited in GAPDH-depleted cells. Caspase activity in A549 cells after transfection with scrambled siRNA (▤) or siGAPDH (▨) and drug treatment was assessed by use of the fluorescence-based caspase 3/7 assay as described under *Materials and Methods* and compared with untreated cells. After transfection, cells were incubated for 48 h and treated with 1 μM DOX for 16 h, or 1 μM araC for 48 h, as indicated under the bar chart. *, $p < 0.05$ compared with no drug treatment. D, induction of the DNA damage marker γH2AX in A549 cells after transfection with scrambled siRNA (▤) or siGAPDH (▨) and drug treatment. After transfection, cells were incubated for 48 h and treated with 1 μM DOX for 16 h, or 1 μM araC for 48 h, as indicated under the bar chart. Cells were harvested in the presence of protease and protein phosphatase inhibitors, and analyzed by Western blot (top blot). β-Actin, loading control. Western blot membrane was quantified by use the Odyssey LI-COR Imaging system, after staining with infrared dye-labeled antibodies (bottom chart). β-Actin was used as the normalization standard. *, $p < 0.05$ compared with no drug control.

nuclear and cytosolic compartments of A549 cells treated with araC and MP. EGFP protein was used as a control in FRAP experiments (Rabut and Ellenberg, 2005). EGFP has been demonstrated to freely diffuse in both nuclear and cytoplasmic compartments; equilibration of the EGFP protein concentration within the nucleus is achieved within 2 s after photobleaching (Wei et al., 2003). Analysis of protein distribution and molecular dynamics of EGFP-GAPDH in the nuclei and cytosol of the cells challenged with genotoxic stress (araC treatment, but not MP) revealed that the nuclear form of EGFP-GAPDH had lower mobility, and the higher fraction of EGFP-GAPDH remained immobilized in the nuclear compartment compared with cytosol (Table 1). In contrast, mobility of EGFP in the nucleus before and after drug treatment remained unaltered. This result indicates that, after araC-induced stress, intranuclear GAPDH becomes involved in molecular interactions with nuclear components. It would be important to characterize both the intranuclear forms of GAPDH and their partners after araC treatment.

Earlier, GAPDH had been demonstrated to contribute to cell cycle regulation via interactions with cyclin B (Carujo et al., 2006) and S-phase-inducible H2B transcription activator OCA-S (Zheng et al., 2003). In our experiments, knockdown of GAPDH induced phosphorylation of Ser 15 in p53, which is a well-established stress marker, thus indicating a functional link between p53 and GAPDH proteins (Fig. 3B and Supplemental Figure S4B). In line with this notion, GAPDH was shown to be up-regulated by p53 after exposure of cerebellar granule cells to apoptotic insult (Chen et al., 1999).

Several pieces of evidence led us to conclude that the cell cycle arrest in GAPDH-depleted cells occurred via activation of the p53-p21 axis: accumulation of GAPDH-depleted cells in G_1 phase occurred in parallel to p53 phosphorylation at Ser 15, p53 stabilization, and accumulation of p53-inducible CDK inhibitor p21 (Fig. 3 and Supplemental Fig. S4), consistent with the classical mechanism of p53-mediated cell cycle arrest (Harper and Brooks, 2005). It is noteworthy that p53-null carcinoma cells NCI-H358 continued proliferation after GAPDH knockdown, although at lower rate, corroborating the hypothesis that p53 is involved in cell cycle arrest in GAPDH-depleted cells (Fig. 3). The slower proliferation of GAPDH-depleted NCI-H358 cells suggests that both glycolytic and regulatory functions of GAPDH are important for cell proliferation. The rescue experiment in which A549 cells

were cotransfected with siGAPDH and siCDKN1A showed that GAPDH- and p21-depleted cells continued proliferating, thus supporting the idea that the cell cycle arrest in GAPDH-depleted cells occurred via p53-induced expression of p21. It is noteworthy that cell cycle arrest in GAPDH-depleted A549 cells was not accompanied by increasing number of apoptotic cells.

Perhaps more important, cell growth arrest occurred in the cells with incomplete GAPDH knockdown (20–25% in A549 cells), and in the abundance of pyruvate in the medium (up to 3 mM). This observation indicates that the cellular level of GAPDH is under strict cellular control.

Despite the cell cycle arrest induced by GAPDH knockdown, incorporation of araC into DNA of the cells with depleted GAPDH occurred at comparable level (Fig. 4B). Therefore, DNA polymerase activity is retained in GAPDH-depleted cells. It was expected, because up to 60% of araC incorporation into DNA occurs by repair synthesis outside DNA replication, as demonstrated by Iwasaki and coauthors (1997).

After araC treatment, GAPDH-proficient cells get arrested in the S phase and proceed to apoptotic death. Depletion of GAPDH in A549 human carcinoma cells caused cell growth arrest, and accumulation of GAPDH-depleted cells in G_0/G_1 phase (Fig. 4). Upon GAPDH depletion, A549 cells accumulate in G_1 phase and do not progress to S phase; correspondingly, araC treatment was not toxic to nondividing cells (Fig. 4A). Because antimetabolites exert their cytotoxic effects in the S phase of the cell cycle (e.g., Brach et al., 1990), and the cell cycle arrest has long been known to have a protective effect against araC-induced cytotoxicity (Tafuri and Andreeff, 1990), our experiments suggest an S-phase-related mechanism of chemoresistance of GAPDH-depleted cells to antimetabolites via activation of p53/p21-controlled cell cycle arrest. Further experiments are warranted to prove this hypothesis. The Comet assay experiments demonstrated that depletion of GAPDH protects DNA from araC-induced damage (Fig. 4C). These results correlate with the decreased formation of γH2AX, a well-established marker of DSB formation (Khanna and Jackson, 2001) (Fig. 5D). In contrast, treatment of A549 cells with DOX did not reveal significant changes in chemosensitivity or DNA damage level in GAPDH-depleted cells consistent with a different cytotoxic mechanism of DOX (Fig. 5, C and D). Down-regulation of GAPDH in Jurkat cells was reported to sensitize cells to prednisolone, a cytotoxic agent with no DNA-damaging effect (Hulleman et al., 2009).

The reduced level of DNA damage and the lower accumulation of γH2AX in the GAPDH-depleted cells after araC treatment support the notion that DSB formation after araC treatment occurs via a cell-cycle-specific biochemical pathway. Reduced DSB and γH2AX formation were in agreement with reduced caspase activation, and increased chemoresistance of GAPDH-depleted cells (Fig. 4C). The latter effect was not noticed in cells treated with doxorubicin (Fig. 5). Instead, DOX treatment caused the comparable levels of DNA damage and γH2AX formed in GAPDH-proficient and -deficient cells. These results suggest that GAPDH does not facilitate γH2AX formation (Fig. 5D).

In conclusion, we demonstrated that, besides its role in the glycolytic energy pathway, GAPDH is a regulator molecule involved in genotoxic stress response. For the first time, we demonstrate that GAPDH depletion induces cell cycle arrest without inducing apoptosis, and resistance to genotoxic drug araC active in the S phase of the cell cycle. Intranuclear form(s) of enzymatically inactive GAPDH bind other nuclear components in response to genotoxic stress. Inhibition of cell growth after GAPDH depletion occurs via a p53-mediated mechanism; knockdown of GAPDH activates p53 and induces accumulation of p21. Identification of GAPDH functions important for cell cycle regulation suggests a strategy to novel inhibitors of cell proliferation, whereas regulation of GAPDH level will open avenues to more precise chemotherapy targeted against DNA in neoplastic cells.

Acknowledgments

We thank Dr. Sachin H. Jadhav for help with RNA interference assay, Nguyen Ngoc for excellent technical assistance, Drs. Patrick J. Piggot and Bettina A. Buttaro (Temple University School of Medicine) for help in performing confocal microscopy and FRAP experiments, and Drs. Salim Merali and Carlos Barrero (Temple University School of Medicine) for helpful discussions and interest in this work.

References

Axelrod D, Koppel DE, Schlessinger J, Elson E, and Webb WW (1976) Mobility measurement by analysis of fluorescence photobleaching recovery kinetics. *Biophys J* **16:**1055–1069.

Azam S, Jouvet N, Jilani A, Vongsamphanh R, Yang X, Yang S, and Ramotar D (2008) Human glyceraldehyde-3-phosphate dehydrogenase plays a direct role in reactivating oxidized forms of the DNA repair enzyme APE1. *J Biol Chem* **283:** 30632–30641.

Brach M, Klein H, Platzer E, Mertelsmann R, and Herrmann F (1990) Effect of interleukin 3 on cytosine arabinoside-mediated cytotoxicity of leukemic myeloblasts. *Exp Hematol* **18:**748–753.

Braess J, Schneiderat P, Schoch C, Fiegl M, Lorenz I, and Hiddemann W (2004) Functional analysis of apoptosis induction in acute myeloid leukaemia-relevance of karyotype and clinical treatment response. *Br J Haematol* **126:**338–347.

Brown VM, Krynetski EY, Krynetskaia NF, Grieger D, Mukatira ST, Murti KG, Slaughter CA, Park HW, and Evans WE (2004) A novel CRM1-mediated nuclear export signal governs nuclear accumulation of glyceraldehyde-3-phosphate dehydrogenase following genotoxic stress. *J Biol Chem* **279:**5984–5992.

Carujo S, Estanyol JM, Ejarque A, Agell N, Bachs O, and Pujol MJ (2006) Glyceraldehyde 3-phosphate dehydrogenase is a SET-binding protein and regulates cyclin B-cdk1 activity. *Oncogene* **25:**4033–4042.

Chen RW, Saunders PA, Wei H, Li Z, Seth P, and Chuang DM (1999) Involvement of glyceraldehyde-3-phosphate dehydrogenase (GAPDH) and p53 in neuronal apoptosis: evidence that GAPDH is upregulated by p53. *J Neurosci* **19:**9654–9662.

Colell A, Ricci JE, Tait S, Milasta S, Maurer U, Bouchier-Hayes L, Fitzgerald P, Guio-Carrion A, Waterhouse NJ, Li CW, et al. (2007) GAPDH and autophagy preserve survival after apoptotic cytochrome c release in the absence of caspase activation. *Cell* **129:**983–997.

Gancedo C and Flores CL (2008) Moonlighting proteins in yeasts. *Microbiol Mol Biol Rev* **72:**197–210.

Hara MR, Agrawal N, Kim SF, Cascio MB, Fujimuro M, Ozeki Y, Takahashi M, Cheah JH, Tankou SK, Hester LD, et al. (2005) S-Nitrosylated GAPDH initiates apoptotic cell death by nuclear translocation following Siah1 binding. *Nat Cell Biol* **7:**665–674.

Harper JV and Brooks G (2005) The mammalian cell cycle, in *Cell Cycle Control* (Humphrey T and Brooks G eds) pp 113–153, Humana Press, Totowa, NJ.

Hulleman E, Kazemier KM, Holleman A, VanderWeele DJ, Rudin CM, Broekhuis MJ, Evans WE, Pieters R, and Den Boer ML (2009) Inhibition of glycolysis modulates prednisolone resistance in acute lymphoblastic leukemia cells. *Blood* **113:**2014–2021.

Iwasaki H, Huang P, Keating MJ, and Plunkett W (1997) Differential incorporation of ara-C, gemcitabine, and fludarabine into replicating and repairing DNA in proliferating human leukemia cells. *Blood* **90:**270–278.

Khanna KK and Jackson SP (2001) DNA double-strand breaks: signaling, repair and the cancer connection. *Nat Genet* **27:**247–254.

Krynetskaia NF, Phadke MS, Jadhav SH, and Krynetskiy EY (2009) Chromatin-associated proteins HMGB1/2 and PDIA3 trigger cellular response to chemotherapy-induced DNA damage. *Mol Cancer Ther* **8:**864–872.

Krynetski EY, Krynetskaia NF, Bianchi ME, and Evans WE (2003) A nuclear protein complex containing high mobility group proteins B1 and B2, heat shock cognate protein 70, ERp60, and glyceraldehyde-3-phosphate dehydrogenase is involved in the cytotoxic response to DNA modified by incorporation of anticancer nucleoside analogues. *Cancer Res* **63:**100–106.

Krynetski EY, Krynetskaia NF, Gallo AE, Murti KG, and Evans WE (2001) A novel protein complex distinct from mismatch repair binds thioguanylated DNA. *Mol Pharmacol* **59:**367–374.

Levine B and Yuan J (2005) Autophagy in cell death: an innocent convict? *J Clin Invest* **115:**2679–2688.

Li Y, Nowotny P, Holmans P, Smemo S, Kauwe JS, Hinrichs AL, Tacey K, Doil L, van

Luchene R, Garcia V, et al. (2004) Association of late-onset Alzheimer's disease with genetic variation in multiple members of the GAPD gene family. *Proc Natl Acad Sci U S A* **101:**15688–15693.
Meyer-Siegler K, Mauro DJ, Seal G, Wurzer J, deRiel JK, and Sirover MA (1991) A human nuclear uracil DNA glycosylase is the 37-kDa subunit of glyceraldehyde-3-phosphate dehydrogenase. *Proc Natl Acad Sci U S A* **88:**8460–8464.
Molina y Vedia L, McDonald B, Reep B, Brüne B, Di Silvio M, Billiar TR, and Lapetina EG (1992) Nitric oxide-induced S-nitrosylation of glyceraldehyde-3-phosphate dehydrogenase inhibits enzymatic activity and increases endogenous ADP-ribosylation. *J Biol Chem* **267:**24929–24932.
Nakajima H, Amano W, Fujita A, Fukuhara A, Azuma YT, Hata F, Inui T, and Takeuchi T (2007) The active site cysteine of the proapoptotic protein glyceraldehyde-3-phosphate dehydrogenase is essential in oxidative stress-induced aggregation and cell death. *J Biol Chem* **282:**26562–26574.
Olive PL, Wlodek D, and Banáth JP (1991) DNA double-strand breaks measured in individual cells subjected to gel electrophoresis. *Cancer Res* **51:**4671–4676.
O'Neil MJ, Smith A, Heckelman PE, and Budavari S, editors (2001) *The Merck Index: An Encyclopedia of Chemicals, Drugs, and Biologicals*, 13th ed, John Wiley & Sons, New York.
Phair RD and Misteli T (2000) High mobility of proteins in the mammalian cell nucleus. *Nature* **404:**604–609.
Rabut G and Ellenberg J (2005) Photobleaching techniques to study mobility and molecular dynamics of proteins in live cells: FRAP, iFRAP, and FLIP, in *Live Cell Imaging* (Goldman RD and Spector DL eds) pp 101–126, Cold Spring Harbor Laboratory Press, Cold Spring Harbor, NY.
Sampath D, Rao VA, and Plunkett W (2003) Mechanisms of apoptosis induction by nucleoside analogs. *Oncogene* **22:**9063–9074.
Sen N, Hara MR, Kornberg MD, Cascio MB, Bae BI, Shahani N, Thomas B, Dawson TM, Dawson VL, Snyder SH, et al. (2008) Nitric oxide-induced nuclear GAPDH activates p300/CBP and mediates apoptosis. *Nat Cell Biol* **10:**866–873.
Sirover MA (2005) New nuclear functions of the glycolytic protein, glyceraldehyde-3-phosphate dehydrogenase, in mammalian cells. *J Cell Biochem* **95:**45–52.
Tafuri A and Andreeff M (1990) Kinetic rationale for cytokine-induced recruitment of myeloblastic leukemia followed by cycle-specific chemotherapy in vitro. *Leukemia* **4:**826–834.
Wei X, Henke VG, Strübing C, Brown EB, and Clapham DE (2003) Real-time imaging of nuclear permeation by EGFP in single intact cells. *Biophys J* **84:**1317–1327.
Xing C, LaPorte JR, Barbay JK, and Myers AG (2004) Identification of GAPDH as a protein target of the saframycin antiproliferative agents. *Proc Natl Acad Sci U S A* **101:**5862–5866.
Zheng L, Roeder RG, and Luo Y (2003) S phase activation of the histone H2B promoter by OCA-S, a coactivator complex that contains GAPDH as a key component. *Cell* **114:**255–266.

Address correspondence to: Dr. Evgeny Krynetskiy, Temple University School of Pharmacy, 3307 North Broad Street, Philadelphia, PA 19140. E-mail: ekrynets@temple.edu